Shock Propagation in Media with Non-uniform Density

Y. Tian, F. Jaberi, and D. Livescu

Abstract Flow resolving shock-capturing and shock-resolving simulations are conducted to study the shock propagation in media with non-uniform density. Shock propagation in a simplified one-dimensional configuration is first examined for various types of density profiles. Both shock-capturing and shock-resolving simulations predict the same results, when there is a separation of scales between the shock width and flow scales. The numerical results agree well with theoretical solutions in the case of weak shocks and linearly varying density fields. In the strong shock limit, better agreement with previous results obtained by the method of characteristics is observed when compared with the theoretical solutions. The differences can be attributed to the effects of re-reflected waves immediately behind the shock, which are not considered in the theoretical solutions. For fluctuating density profiles, the numerical results further deviate from the theoretical solutions and exhibit additional long-wavelength oscillations, which are shown to be related to the re-reflected waves. 3D density variations, with and without turbulent velocity fluctuations, are also considered to examine the shock propagation in flows with strongly variable complex density fields.

1 Introduction

When a normal shock wave propagates through a non-uniform medium, the strength and geometry of the shock wave, as well as the medium itself, will be modified through their interactions. This is an important fundamental problem in the study of inertial confinement fusion (ICF), supersonic and hypersonic combustion, astrophysics, and other applications [1, 2]. In an early theoretical study [3],

Y. Tian · F. Jaberi
Michigan State University, East Lansing, MI, USA

D. Livescu (✉)
Los Alamos National Laboratory, Los Alamos, NM, USA
e-mail: livescu@lanl.gov

A. Sasoh et al. (eds.), *31st International Symposium on Shock Waves 1*,
https://doi.org/10.1007/978-3-319-91020-8_141

Chisnell investigated the one-dimensional propagation of shock waves through a non-uniform (variable density) medium and derived an expression for the shock Mach number as a function of time. Later, Whitham [4] developed a more general analytical solution for a medium with both varying density and pressure. These earlier formulations of shock propagation, even though useful, suffer from a number of difficulties, one of which originates from the fact that the re-reflected waves immediately after the shock are ignored. The re-reflected wave effects are accounted for in the study conducted by Bird [5], who performed numerical simulations with the method of characteristics and compared them with the Chisnell-Whitham (as referred to in [5]) results and asymptotic solutions. Soukhomlinov et al. [6] further examined the effects of temperature gradients on shock propagation. Their results were in good agreement with Bird's results. The early experimental study by Hesselink and Sturtevant [2] has considered weak shock propagation through a random medium. These studies were further extended to more complex problems [1, 2]. However, there has been little effort to extend the early theories, simulations, or experiments to describe shock propagation in variable density turbulence.

The canonical interaction between a normal shock wave and isotropic turbulence (the canonical shock-turbulence interaction problem or STI) is an example of shock propagation in non-uniform media (Fig. 1). Here, the non-uniformity in the pre-shock region is mainly due to turbulent motions. In this type of problem, the shock propagation can reach a quasi-steady state for a range of parameters so that the statistical behavior of turbulence through the shock or in the post-shock region is of interest. Such a flow has been studied using experiments, full DNS, shock-capturing

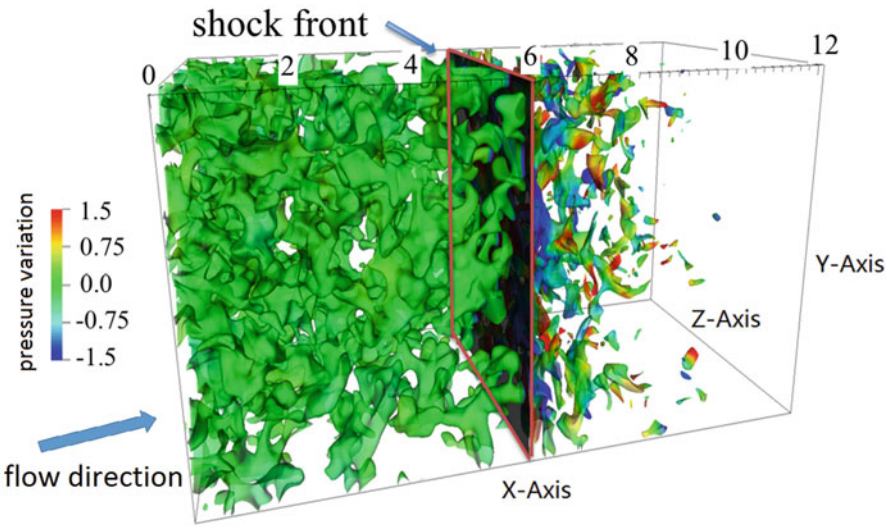

Fig. 1 Pressure contours in a Mach 2 shock-isotropic turbulence configuration

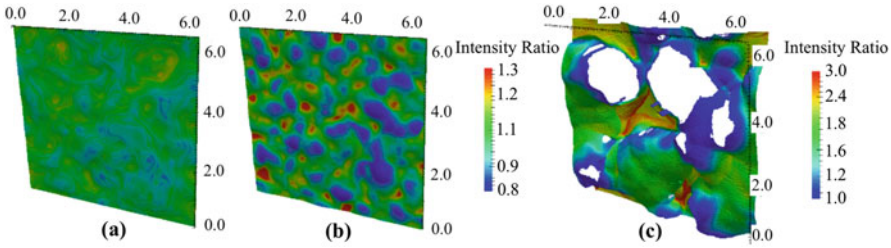

Fig. 2 Shock front in wrinkled shock regime (**a**, **b**) and broken shock regime (**c**). Shock intensity is represented by density jump $\Delta\rho$. Shock intensity ratio is calculated as $\Delta\rho/\overline{\Delta\rho}$

simulations, and analytical analysis of limiting cases [7–9]. However, there are only few studies on turbulence modification of shock propagation.

Recently, our group has investigated the shock interaction with variable density turbulence and has shown that shock front, shock intensity, and post-shock turbulence are strongly affected (Fig. 2a, b) by the non-uniformities in density, even at low-density ratios [10, 11]. By further increasing the density ratio, the interaction exhibits a broken shock regime similar to the effect seen at high M_t values [7] (Fig. 2c). In previous studies, the interaction was studied in regimes where the shock motion was negligible [8] or the constant back pressure outflow condition was used to stabilize the shock motion even at high M_t values or density ratios [7] so that the statistical analysis could be carried out. In this study, the transient shock propagation in variable density turbulence without boundary effects is of interest, as it resembles the conditions considered in the early theoretical work and practical applications of interest (e.g., ICF). We aim to test the available theories on predicting the shock wave and post-shock flow under various conditions using a simplified pseudo-1D configuration and then investigate the 3D shock propagation in variable density turbulent flows.

The computational setup and numerical methods are described in the next section, before discussing the numerical results. Pseudo-1D simulations are conducted first for flows with several types of density field variations. The numerical results are compared with those obtained by early theoretical models and more advanced models. Then, 3D simulations are conducted to understand the 3D density and turbulence effects on shock propagation. The main findings and conclusions are summarized in the last section.

2 Computational Setup and Numerical Methods

In this section, details of the numerical methods and computational setup are described for pseudo-1D and 3D simulations. For both cases, we have performed both shock-resolving and shock-capturing simulations to ensure the accuracy of the results. The bulk of the results are obtained using a high-order hybrid numerical

method solving the conservative form of the dimensionless compressible Navier-Stokes equations for continuity, momentum, energy, and mass fraction. The inviscid fluxes are computed by the fifth-order Monotonicity-Preserving (MP) scheme as described in [12], and the viscous fluxes are computed using the sixth-order compact scheme. The third-order Runge-Kutta scheme is used for time advancement. The accuracy of the scheme has been verified in [12] for various types of compressible flows and in [10, 11] for STI. Shock-resolving simulations are also conducted to verify the accuracy of shock-capturing simulations in predicting shock movement. For this, the sixth-order compact finite differences are used for both viscous and inviscid fluxes. To fully resolve all flow scales, including shock width (δ), the mesh is further refined around the shock region. At least 12 grid points are used in the streamwise direction to resolve the shock profile, in contrast to the shock-capturing simulations, where the shock wave is numerical and is represented by only two to three grid points.

The physical domain for the 3D shock propagation simulations is a box that has dimensions of 4π in the streamwise direction and 2π in the transverse directions (Fig. 1). The coordinate system follows the initial normal shock motion. The boundary conditions and generation of the inflow fields are explained in [10, 11]. For the pseudo-1D simulations, all the variations in transverse directions including density and turbulence variations are removed. Constant pressure, velocity, and temperature inflow conditions are imposed, and only the density is allowed to vary in the streamwise direction by changing the mole fractions of the fluids in the mixture. The inflow conditions resemble those in Refs. [3–5]. For all simulations, the outflow boundary conditions have no effect on the shock wave. This has been tested by using different buffer layer and computational domain lengths, and the results show that the shock motion is not affected by the outflow boundary conditions.

3 Results and Discussion

3.1 Shock Wave Propagation in Media with Linearly Varying Density

In this section, the simple case of shock propagation in a linearly varying density field is considered. The aim is to verify the accuracy of current shock-capturing simulations in predicting shock propagation in variable density media. Pseudo-1D simulations in the weak shock limit of $M_0 = 1.1$ with density ratios of 8 and 0.125 are performed first. Figure 3a compares the time development of shock position obtained from numerical results and Chisnell-Whitham theory (C-W solution). The x-axis denotes time, and the upper curve and lower curve represent cases with increasing and decreasing density field, respectively. As observed, in the weak shock limit, the results from current shock-capturing simulations are in excellent agreement with the C-W solution for both decreasing and increasing

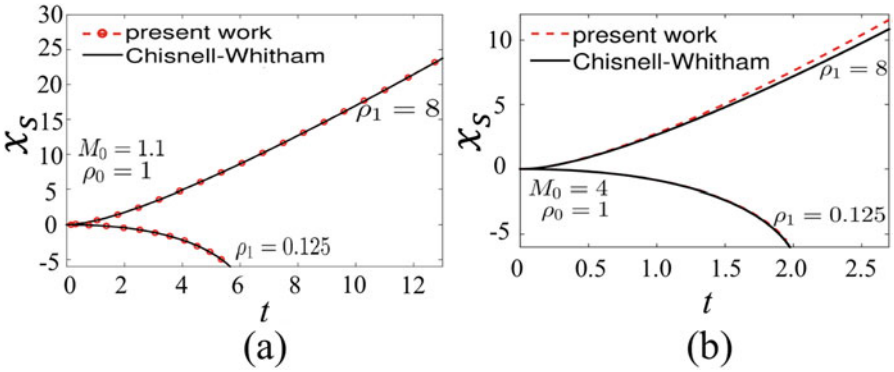

Fig. 3 Shock wave propagation in the medium with linearly varying density for density ratios of 8 and 0.125. (**a**) $M_0 = 1.1$ and (**b**) $M_0 = 4$

density profiles. On the other hand, the match with the C-W solution is less than satisfactory for a strong shock ($M_0 = 4$). In this case, the numerical results for the case with increasing density gradually deviate from the C-W solution in time (Fig. 3b), resulting in a final difference of around 5%. The case with decreasing density shows a relatively better agreement at $M_0 = 4$.

To further understand the discrepancy, we compare the results from current simulations with those obtained by Bird [5], who used the method of characteristics. The exact same conditions are used in Ref. [5], for Mach number 4.0 and density ratios of 8 and 0.125. The comparison of the shock Mach number as a function of distance is shown in Fig. 4. Evidently, the current results agree better with those obtained by the method of characteristics for the increasing density case. On the other hand, for the linearly decreasing density case, all three methods give comparable predictions. It was argued in Ref. [5] that the influence of re-reflected waves, which is not considered in the C-W solution, is different for different density profiles. This explains the different performance of the C-W model in different situations. Our numerical results agree well with those obtained by the method of characteristics and also with C-W theory when the re-reflected waves are not important.

3.2 Shock Wave Propagation in Medium with Fluctuating Density

In this section, the shock propagation in a medium with a fluctuating density field is studied. The shock is initialized in a fluid with $\rho = 1.0$; then a fluid with density profile given by $\rho = 1.0 + (1 - A_t)/(1 + A_t)\sin(k_s x)$ is superposed on the mean flow, where A_t is the Atwood number. By following this procedure, the mean density

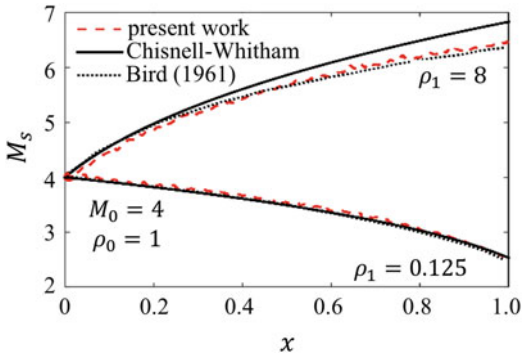

Fig. 4 Evolution of shock Mach number in linearly varying density field for $\rho_1/\rho_0 = 8$ and 0.125 ($M_0 = 4$)

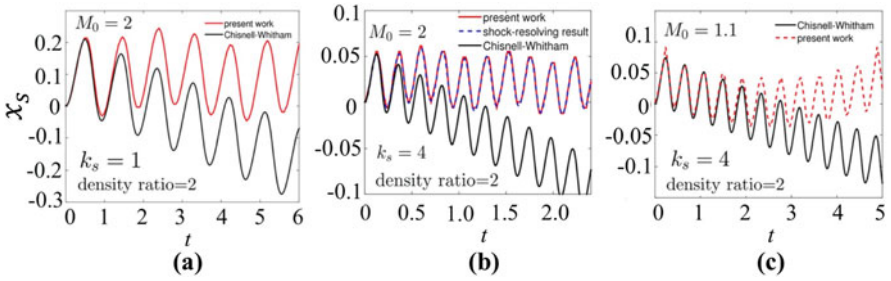

Fig. 5 Shock propagation in a fluctuating density field. (**a**, **b**) $M_0 = 2.0$, density ratio 2.0, and $k_s = 1$ and $k_s = 4$ and (**c**) $M_0 = 1.1$, density ratio 2.0, and $k_s = 4$

ahead of the shock is still one ($\overline{\rho} = 1.0$). The numerical results are compared with the C-W solution to test the applicability of the model to such density variations.

In Fig. 5a, b, the temporal development of shock position is shown for a Mach 2 shock and small density ratio of 2:1 ($A_t = 0.33$) at different wavenumbers of $k_s = 1$ and 4. As shown, the C-W solution predicts a shock motion that resembles the sine wave variation in the density profile but with a constant mean velocity relative to the unperturbed shock that moves the shock wave upstream. The match between the numerical and theoretical solution is fairly good during the first (sine) wave cycle. However, after the first cycle, the shock wave acquires additional oscillatory motions instead of moving upstream following the original sine wave with a constant mean velocity, as predicted by the theory. Thus, the current shock-capturing simulations are predicting long-wavelength oscillatory motions superposed on the original sinusoidal motion. Shock-resolving simulations are also conducted to verify this observation. As seen in Fig. 5b, shock-resolving results match very well with the shock-capturing results, proving that the deviation from C-W solution and the long-wavelength oscillatory motions are both physical. The ratio of the wavenumber, k_l, of the first harmonic of these long-wavelength motions to the sine wave wavenumber, k_s, is denoted as $r_l = \frac{k_l}{k_s} \approx 1/4$. This ratio appears to be the same for $k_s = 1$ and 4. To explain these long-wavelength motions, we consider two velocities that are related to the behavior of shock: (1) the velocity at

which the pre-shock medium approaches the shock wave v_p and (2) the velocity of the re-reflected waves approaching the shock wave, v_r, relative to the shock speed. v_p carries the density fluctuations responsible for moving the shock wave. v_r can be found from the local sound speed behind the shock. The re-reflected waves can eventually overtake the initial shock and affect its strength and speed [5]. The ratio of v_r/v_p is denoted as r_v and we find that $r_v \approx r_l$. For a weaker shock, as shown in Fig. 5c, r_v and r_l have small magnitudes: $r_v \approx r_l \approx 1/12$. Thus, the early time agreement with the C-W model is improved, and the long-wavelength variation in shock position is also clearer. It can be inferred that the re-reflected waves causing the long-wavelength motions of the shock [5] are responsible for the deviation from the theoretical solution. For a fluctuating density profile, it seems that the re-reflected waves play a more important role in changing the shock strength and the shock motion, further deviating from the C-W model.

3.3 Shock Wave Propagation in Three-Dimensional Non-uniform Density Media

It has been shown above that in a medium with linearly increasing or decreasing density, the C-W solutions give reasonable prediction, in the weak shock limit. However, when significant density fluctuations around the mean are included, the ability of accounting for the re-reflected waves becomes necessary, making the C-W solution less accurate. In this section, we take a step further to extend the simulation to three-dimensional configurations approaching more practical applications.

Two different 3D simulations are conducted: Mach 2 shock propagating in (1) highly non-uniform density field with turbulence and (2) in non-uniform density field without turbulence. The plane shock is wrinkled by the non-uniform density field; therefore the shock position is calculated as the mean position over the whole shock surface. For the turbulence simulations, the turbulent Mach number is $M_t = 0.09$, and Taylor Reynolds number is $Re_\lambda = 30$. The scalar spectrum used to generate the density field is peaked at $k_s = 4$. The numerical results are compared with those obtained using the C-W model in Fig. 6. In the 3D turbulent simulation, the shock propagation is slower by about 5% compared to the case without turbulence, implying that the shock motion is mainly caused by the density non-uniformity and not the turbulence. The C-W solution provides a reasonably good approximation for the shock propagation, despite the large differences when comparing with the pseudo-1D simulation with fluctuating (sinusoidal) density field shown above. In the 3D simulation, it appears that more complicating effects, like the shock front distortion, cancel some of the 1D wave re-reflection effects seen above. To better understand the 3D density variations and turbulence on the shock wave, more detailed studies are needed. Further work will be focused on examining local shock motion and distortion using 3D shock dynamics to understand the averaged shock behavior.

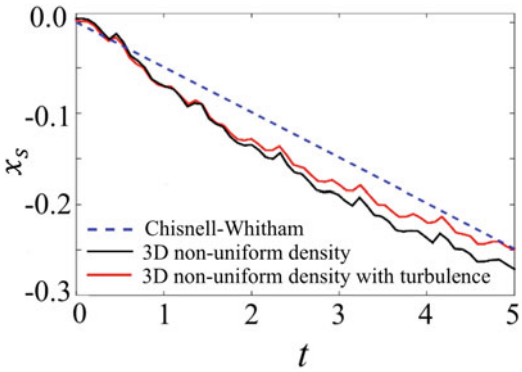

Fig. 6 Shock propagation in a 3D density field. $M_0 = 2.0$, density ratio of 2.0, and $k_s = 4$

4 Conclusions

Flow resolving shock-capturing and shock-resolving simulations have been conducted to study shock propagation in non-uniform density media. The main objective is to understand the variable density effects on shock wave propagation and post-shock flow. First, simplified pseudo-1D simulations are conducted for various types of density fields. Results show that at low shock strengths, the numerical results agree well with those obtained by the C-W model for linearly varying density. For strong shocks, however, the computational results are closer to those obtained using the method of characteristics, which considers the re-reflected waves. For a density field that follows a sine wave pattern, the shock motion deviates from the C-W predictions and exhibits additional long-wavelength oscillations in both shock-capturing and shock-resolving simulations. The first harmonic of these oscillations appears related to the re-reflected waves, which are not considered in the C-W model. The analysis is then extended to study shock propagation in a medium with significant 3D density fluctuations, with and without turbulence. The shock motion seems to be dominated by the density variations and not very much affected by the relatively weak turbulence considered in this study. More interestingly, the agreement with the C-W solution appears to be better in the 3D configuration, when compared to the case with only 1D density fluctuations. This suggests that the introduction of more complicating effects in the 3D simulations with highly non-uniform density and turbulence may overshadow the re-reflected wave effects.

References

1. D. Ranjan et al., Shock-bubble interactions. Annu. Rev. Fluid Mech. **43**, 117 (2011)
2. L. Hesselink, B. Sturtevant, J. Fluid Mech. **196**, 513 (1988)
3. R.F. Chisnell, Proc. R. Soc. A **232**, 350 (1955)
4. G.B. Whitham, J. Fluid Mech. **4**, 337 (1958)
5. G.A. Bird, J. Fluid Mech. **11**, 180 (1961)

6. V.S. Soukhomlinov et al., Formation and propagation of a shock wave in a gas with temperature gradients. J. Fluid Mech. **473**, 245 (2002)
7. J. Larsson et al., Reynolds- and Mach-number effects in canonical shock-turbulence interaction. J. Fluid Mech. **717**, 293 (2013)
8. J. Ryu, D. Livescu, J. Fluid Mech. **756**, R1 (2014)
9. D. Livescu, J. Ryu Shock Waves **26**, 241 (2016)
10. Y. Tian et al., Numerical study of variable density turbulence interaction with a normal shock wave, J. Fluid Mech. **829**, 551–588 (2017)
11. Y. Tian et al., Numerical simulation of multi-fluid shock-turbulence interaction. AIP Conf. Proc. **1793**, 150010 (2017)
12. Z. Li, F.A. Jaberi, Int. J. Numer. Meth. Fl. **68**, 740 (2012)